New implementation of second-order Møller-Plesset perturbation theory with an analytic Slater-type geminal

Seiichiro Ten-no
Graduate School of Information Science, Nagoya University, Chikusa-ku, Nagoya 464-8601, Japan and CREST, Japan Science and Technology Agency (JST), 4-1-8 Honcho Kawaguchi, Saitama 332-0012, Japan

(Received 11 October 2006; accepted 8 November 2006; published online 5 January 2007)

The author introduces a new method for the exchange commutator integrals in explicitly correlated Møller-Plesset second order perturbation theory. The method is well suited with an analytic Slater-type geminal correlation factor. He also explains the scheme for auxiliary integrals needed for the correlation factor. Based on different *Ansätze*, he analyzes the performance of the method on correlation energies and reaction enthalpies in detail. © *2007 American Institute of Physics*.
[DOI: 10.1063/1.2403853]

I. INTRODUCTION

Most of the standard correlated methods in *ab initio* electronic structure theory converge very slowly as $(L_{\max}+1)^{-3}$ with the maximum angular momentum of one-electronic basis $L_{\max}$. This is due to the inability of describing the cusps at coalescence in the exact wave function[1–3] in terms of the products of one-particle basis functions. Ever since it was found that the inclusion of a linear-r_{12} term accelerates the convergence of a configuration interaction (CI) expansion substantially,[4] the use of basis functions explicitly dependent on the interelectronic distance has drawn a considerable attention in quantum chemistry. The explicitly correlated Gaussian-type functions introduced by Boys[5] and Singer[6] have been plugged into many-electron theories feasibly as Gaussian-type geminals (GTG).[7–9] These methods, however, require at least three-electron integrals and the applicability is limited to small molecules.

The R12 methods were introduced to overcome these difficulties.[10,11] The use of a linear-r_{12} basis ensures the convergence in $(L_{\max}+1)^{-7}$.[10,11] More importantly, the resolution of the identity (RI) side-steps the calculation of many-electron integrals explicitly by expanding a many-electron integral into a sum of products of two-electron integrals.[11] These features have made it possible to obtain accurate energies at reasonable computational costs. A large basis set must be employed to ensure the accuracy of the RI approximation. Nevertheless, Klopper and Samson introduced auxiliary basis set[12] (ABS) to enable us to use standard orbital basis sets such as Duning's correlation consistent series.[13–15] Recent works have been focused on improving the performance and accuracy through the density fitting (DF),[16] a hybrid RI and ABS approach,[17] and better RI approximations using the combined DF/RI method[18] and complementary ABS.[19] It has been shown that the alternative method using a numerical quadrature[20] (QD) improves both of the aspects simultaneously.

More recently, we proposed the use of a Slater-type geminal (STG) correlation factor[21] $\exp(-\zeta r_{12})$ in explicitly correlated theory in place of linear r_{12} or GTG. It turned out that the exponential factor leads to excellent results. Right after, other authors have reported confident results that STG outperforms other correlation factors[22] and the main source of the error in explicitly correlated methods is the choice of the correlation factor.[23] The STG correlation factor has been employed successfully in various applications of the Møller-Plesset second order perturbation theory (MP2)-F12 methods[24–26] that use a factor other than linear r_{12}. The exponential correlation factor is also supported by a rather recent mathematical study of Fournais *et al.*[27] Readers can refer to an overview of the current status of the field in the recent review article.[28]

The main purpose of this paper is twofold. The first one is to develop an efficient method based on QD to compute the exchange commutator integrals needed in the MP2-F12/B methods. These objects are of four-electron integrals. The second purpose is to improve the efficiency of the computation of STG integrals. In what follows, we present necessary formulas. Numerical results involving reaction enthalpies are presented in Sec. III.

II. THEORY

A. MP2-F12 formulation with cusp conditions

Henceforward, we denote orthonormalized occupied, virtual, and general orbitals in a given basis set as $ij\ldots$, $ab\ldots$, and $pq\ldots$, respectively. The exact wave function obeys the s- and p-wave cusp conditions for singlet and triplet pairs, respectively.[1–3] In our MP2-F12 methods using the cusp conditions explicitly, the singlet ($s=0$) and triplet ($s=0$) spinless parts of the pair functions are

$$\tilde{u}_{ij}^{(s)} = c_{ij}^{ab}(s)\{ab\}^{(s)} + \chi_{ij}^{(s)}, \tag{1}$$

$$\chi_{ij}^{(s)} = \frac{1}{1+s}\hat{Q}_{12}f_{12}\{ij\}^{(s)}, \tag{2}$$

where $\hat{Q}_{12}$ is the usual strongly orthogonal projector,[7]

$$\hat{Q}_{12} = (1 - \hat{O}_1)(1 - \hat{O}_2), \tag{3}$$

with the projection operator onto the occupied orbitals,

$$\hat{O}_n = \sum_i |\varphi_i(n)\rangle\langle\varphi_i(n)|, \tag{4}$$

and the symmetrized and antisymmetrized orbital products are

$$\{pq\}^{(0)}(\mathbf{r}_1,\mathbf{r}_2) = \delta_{pq}\varphi_p(\mathbf{r}_1)\varphi_q(\mathbf{r}_2) + \frac{1}{\sqrt{2}}(1-\delta_{pq}) \times[\varphi_p(\mathbf{r}_1)\varphi_q(\mathbf{r}_2) + \varphi_q(\mathbf{r}_1)\varphi_p(\mathbf{r}_2)], \tag{5}$$

$$\{pq\}^{(1)}(\mathbf{r}_1,\mathbf{r}_2) = \frac{1}{\sqrt{2}}[\varphi_p(\mathbf{r}_1)\varphi_q(\mathbf{r}_2) - \varphi_q(\mathbf{r}_1)\varphi_p(\mathbf{r}_2)]. \tag{6}$$

The use of the projector [Eq. (3)] is labeled as *Ansatz* 2 to be distinguished from *Ansatz* 1 with the projector onto the given orbitals,

$$\hat{P}_n = \sum_p |\varphi_p(n)\rangle\langle\varphi_p(n)|, \tag{7}$$

instead of $\hat{O}_n$ that has been conveniently employed in conjunction with RI. Nowadays the main current rests on the methods beyond the standard approximation and *Ansatz* 1 is less accurate. Thus the classification is just a historical meaning,[28] and we use *Ansatz* 2 without labeling our methods. In this work, we use a STG correlation factor,

$$f_{12} = f_{12}^{(\mathrm{STG})} \equiv -\frac{r_c}{2}\exp\left(-\frac{r_{12}}{r_c}\right), \tag{8}$$

with a length scale parameter r_c. It is possible to fit a linear combination of GTG with STG,[21–23] yet the analytical treatment is more efficient as shown later. The dependency of the coefficient on s in $\chi_{ij}^{(s)}$ can be removed in terms of the rational generator with a permutation operator.[20] This feature is particularly important for the treatment of multireference wave functions in an internally contracted manner.[29]

The second order energy is

$$E^{(2)} = \sum_{s=0,1}(2s+1)\sum_{i\geqslant j}(e_{ij}^{(s)} + d_{ij}^{(s)}), \tag{9}$$

where $e_{ij}^{(s)}$ are the usual pair energies,

$$e_{ij}^{(s)} = \frac{1}{1+\delta_{ij}}\sum_{ab}\frac{\langle ij|ab\rangle\langle ab|ij\rangle^{(s)}}{\varepsilon_i+\varepsilon_j-\varepsilon_a-\varepsilon_b}, \tag{10}$$

with

$$|pq\rangle^{(s)} = |pq\rangle + (1-2s)|qp\rangle, \tag{11}$$

and $d_{ij}^{(s)}$ are contributions from the correlation factor,

$$d_{ij}^{(s)} = -\tilde{B}_{ij}^{(s)} + 2\tilde{V}_{ij}^{(s)}, \tag{12}$$

$$\tilde{B}_{ij}^{(s)} = \frac{1}{(1+\delta_{ij})(1+s)^2}B_{ij}^{(s)}, \tag{13}$$

$$\tilde{V}_{ij}^{(s)} = \frac{1}{(1+\delta_{ij})(1+s)}V_{ij}^{(s)}. \tag{14}$$

The constituting elements are

$$B_{ij}^{(s)} = \langle ij|[\hat{F}_{12},f_{12}]\hat{Q}_{12}f_{12}|ij\rangle^{(s)} - \sum_{ab}\phi_{ij}^{ab}\langle ij|[\hat{F}_{12},f_{12}]|ab\rangle^{(s)}, \tag{15}$$

$$V_{ij}^{(s)} = \langle ij|r_{12}^{-1}\hat{Q}_{12}f_{12}|ij\rangle^{(s)} - \sum_{ab}\phi_{ij}^{ab}\langle ij|r_{12}^{-1}|ab\rangle^{(s)}, \tag{16}$$

$$\phi_{ij}^{ab} = \frac{\langle ab|[\hat{F}_{12},f_{12}]|ij\rangle}{\varepsilon_a+\varepsilon_b-\varepsilon_i-\varepsilon_j}, \tag{17}$$

and the Fock operator is $\hat{F}_{12}=\hat{F}_1+\hat{F}_2$. For ϕ_{ij}^{ab}, we have used the generalized Brillouin condition (GBC), that assumes the exactness of the occupied orbitals in the complete basis set (CBS) limit to lead to

$$[\hat{F}_{12},\hat{Q}_{12}] \overset{\mathrm{GBC}}{\cong} 0. \tag{18}$$

According to the decomposition of the commutator into the kinetic ($\hat{T}_{12}=\hat{T}_1+\hat{T}_2$) and exchange ($\hat{K}_{12}=\hat{K}_1+\hat{K}_2$) energy operator components,

$$[\hat{F}_{12},f_{12}] = [\hat{T}_{12},f_{12}] - [\hat{K}_{12},f_{12}], \tag{19}$$

the $\mathbf{B}^{(s)}$ matrix is expressed as

$$\mathbf{B}^{(s)} = \mathbf{T}^{(s)} + \mathbf{P}^{(s)} - \mathbf{Q}^{(s)}, \tag{20}$$

$$T_{ij}^{(s)} = \langle ij|[\hat{T}_{12},f_{12}]\hat{Q}_{12}f_{12}|ij\rangle^{(s)} - \sum_{ab}\phi_{ij}^{ab}\langle ij|[\hat{T}_{12},f_{12}]|ab\rangle^{(s)}, \tag{21}$$

$$P_{ij}^{(s)} = \langle ij|f_{12}\hat{K}_{12}\hat{Q}_{12}f_{12}|ij\rangle^{(s)} - \sum_{ab}\phi_{ij}^{ab}\langle ij|f_{12}\hat{K}_{12}|ab\rangle^{(s)}, \tag{22}$$

$$Q_{ij}^{(s)} = \langle ij|\hat{K}_{12}f_{12}\hat{Q}_{12}f_{12}|ij\rangle^{(s)} - \sum_{ab}\phi_{ij}^{ab}\langle ij|\hat{K}_{12}f_{12}|ab\rangle^{(s)}. \tag{23}$$

The accuracy of Eq. (2) at finite r_{12} is partially indicated by the measure,

$$M_{ij}^{(s)} = \frac{\tilde{V}_{ij}^{(s)}}{\tilde{B}_{ij}^{(s)}}, \tag{24}$$

which gives the optimum energy within the framework of the diagonal (*IJIJ*) *Ansatz* as

$$\chi_{ij}^{(s)}(IJIJ) = c_{ij}^{(s)}\hat{Q}_{12}f_{12}\{ij\}^{(s)}, \tag{25}$$

$$d_{ij}^{(s)}(IJIJ) = M_{ij}^{(s)}\tilde{V}_{ij}^{(s)}. \tag{26}$$

$d_{ij}^{(s)}$ (*IJIJ*) is not unitary invariant over occupied orbitals, and this drawback can be resolved by the addition of the off-diagonal (*IJKL*) contribution in pair functions,[30]

TABLE I. Properties of the *Ansätze*.

	SP	*IJIJ*	*IJKL*
Size-consistency	Yes (F12)	Yes (F12)	Yes
Unitary invariance	Yes	No	Yes
Correctness at coalescence	Yes	No	No
Additivity	Yes	Yes	Yes (fixed *KL* space)
Size of the final intermediates	O^2	O^2	O^6 (O^8)

$$\chi_{ij}^{(s)}(IJKL) = \sum_{k\geqslant l} c_{ij}^{kl(s)} \hat{Q}_{12} f_{12} \{kl\}^{(s)}. \tag{27}$$

The main properties of the *Ansatz* with the *s*- and *p*-wave (*SP*) cusp conditions [Eq. (2)] and those of *IJIJ* [Eq. (25)] and *IJKL* [Eq. (27)] are summarized in Table I. The SP and *IJIJ Ansätze* are size-inconsistent for the linear-r_{12} correlation factor with canonical orbitals. This is an artificial deficiency due to the factor which does not die away. Both of the *Ansätze* fulfill the size-consistency for a short-ranged F12 factor. Unlike *IJIJ*, more simplified SP retains the unitary invariance. The coefficient $1/(1+s)$ in $\chi_{ij}^{(s)}$ is a consequence of *SP* that ensures the elimination of the singularity of the perturbation at coalescence explicitly both for the singlet and triplet pairs.[1–3] Because of the numbers of amplitudes regarding F12, correlation energy is in the order, $IJKL < IJIJ < SP$. The *IJIJ* and *IJKL Ansätze*, however, lead to a deviation from the exact slope in the correlation factor at coalescence, and the singularity can removed only in the CBS limit numerically. In the unitary invariant (*IJKL*) formulation, the additivity of correlation energy is fulfilled only when we use a fixed set of *KL* pairs irrespective of the choice of correlated *IJ* pairs. The sizes of the final objects for correlation energies are O^2 in *SP* and *IJIJ* and O^6 in the *IJKL Ansatz* for the number of occupied orbitals *O*. In addition, the diagonalization process costs O^8 operations in *IJKL*, while this is not the rate-determining step usually unless *O* is very large. The *IJIJ* and *SP Ansätze* are generally more stable than *IJKL* numerically (for numerical stability, see, for instance, Ref. 31).

B. Computer implementation

Several approximations have been introduced in practical implementations of explicitly correlated electronic structure theory. The extended Brillouin condition (EBC) assumes that the Fock operator is closed in the orbital space to simplify Eq. (17) as

$$\phi_{ij}^{ab} \overset{\text{EBC}}{\cong} f_{ij}^{ab}. \tag{28}$$

A method with EBC is distinguished by appending an asterisk. It has been discussed that the contribution of $\mathbf{P}^{(s)}$ is negligibly small.[11,12,17] Actually, $\mathbf{P}^{(s)}$ vanishes in the standard approximation with EBC. The MP2-F12/A method drops both $\mathbf{P}^{(s)}$ and $\mathbf{Q}^{(s)}$ in Eq. (20),

$$\mathbf{B}^{(s)} \overset{\text{A}}{\cong} \mathbf{T}^{(s)}, \tag{29}$$

while MP2-F12/B retains $\mathbf{Q}^{(s)}$,

$$\mathbf{B}^{(s)} \overset{\text{B}}{\cong} \mathbf{T}^{(s)} - \mathbf{Q}^{(s)}. \tag{30}$$

We also examined the effects of EBC to $\mathbf{P}^{(s)}$ numerically,

$$\Delta P_{ij}^{(s)} = -\sum_{ab} (\phi_{ij}^{ab} - f_{ij}^{ab}) \langle ij|f_{12}\hat{K}_{12}|ab\rangle^{(s)}, \tag{31}$$

which turned out to be negligibly small indeed. The matrix $\mathbf{Q}^{(s)}$ contributes positively to the correlation energy, and the approximation "A" does not necessarily give an upper bound of the true MP2 energy. In Ref. 20, all expressions needed in MP2-F12/A*, that is of Eqs. (28) and (29), are derived in terms of QD. We present additional formulae in regard to ϕ_{ij}^{ab} and $\mathbf{Q}^{(s)}$ hereafter.

ϕ_{ij}^{ab} is divided into the contributions of the kinetic and exchange energy operators,

$$\phi_{ij}^{ab} = \frac{\langle ab|[\hat{T}_{12}, f_{12}]|ij\rangle - \langle ab|[\hat{K}_{12}, f_{12}]|ij\rangle}{\varepsilon_a + \varepsilon_b - \varepsilon_i - \varepsilon_j}. \tag{32}$$

The integrals $\langle ab|[\hat{T}_{12}, f_{12}]|ij\rangle$ can be calculated analytically, while $\langle ab|[\hat{K}_{12}, f_{12}]|ij\rangle$ are actually of three-electron integrals and are expressed in terms of a numerical quadrature as

$$\langle ab|[\hat{K}_1, f_{12}]|ij\rangle = \sum_g [(X_{ai}(\mathbf{r}_g) - X_{ai}^{+}(\mathbf{r}_g)\ ]\langle b|f_{1g}|j\rangle, \tag{33}$$

where

$$X_{pq}(\mathbf{r}_g) = K_p(\mathbf{r}_g)\bar{\varphi}_q(\mathbf{r}_g), \tag{34}$$

$K_p(\mathbf{r}_g)$ are the exchange operators in the physical space,

$$K_p(\mathbf{r}_g) = \sum_i \langle p|r_{1g}^{-1}|i\rangle \varphi_i(\mathbf{r}_g), \tag{35}$$

and $\bar{\varphi}_p(\mathbf{r}_g)$ are orbital amplitudes multiplied by the quadrature weight at $\mathbf{r}_g$,

$$\bar{\varphi}_p(\mathbf{r}_g) = w(\mathbf{r}_g)\varphi_p(\mathbf{r}_g). \tag{36}$$

For $\mathbf{Q}^{(s)}$, we expand Eq. (23) as

$$Q_{ij}^{(s)} = \langle ij|\hat{K}_{12}f_{12}^2|ij\rangle^{(s)} - \langle ij|\hat{K}_{12}f_{12}(\hat{O}_1 + \hat{O}_2)f_{12}|ij\rangle^{(s)} + \langle ij|\hat{K}_{12}f_{12}\hat{O}_1\hat{O}_2 f_{12}|ij\rangle^{(s)} - \sum_{ab} \phi_{ij}^{ab}\langle ij|\hat{K}_{12}f_{12}|ab\rangle^{(s)}. \tag{37}$$

The last two terms can be calculated by a formula analogous to Eq. (33), and the first term is

$$\langle ij|\hat{K}_{12}f_{12}^2|kl\rangle = \sum_g [X_{ik}(\mathbf{r}_g)\langle j|f_{1g}^2|l\rangle + X_{jl}(\mathbf{r}_g)\langle i|f_{1g}^2|k\rangle], \tag{38}$$

that requires the integrals over the operator f_{12}^2. Nevertheless, it is not necessary to calculate these integrals explicitly in the STG case since the operator is related with the one in the MP2-F12/A method as

$$(f_{12}^{(\mathrm{STG})})^2 = r_c^2(\nabla_1 f_{12}^{(\mathrm{STG})})\cdot(\nabla_1 f_{12}^{(\mathrm{STG})}). \tag{39}$$

The remaining term in Eq. (37) is divided as

$$\langle ij|\hat{K}_1 f_{12}(\hat{O}_1+\hat{O}_2)f_{12}|ij\rangle^{(s)} = \langle ij|\hat{K}_1 f_{12}\hat{O}_1 f_{12}|ij\rangle^{(s)} + \langle ij|\hat{K}_1 f_{12}\hat{O}_2 f_{12}|ij\rangle^{(s)}. \tag{40}$$

The second term is actually of four-electron integrals in which the first coordinate is shared by the triplicated two-electron operators, i.e., a couple of f_{12} and r_{12}^{-1} in $\hat{K}_1$. These special kind of four-electron integrals can be calculated with QD explicitly as

$$\langle ij|\hat{K}_1 f_{12}\hat{O}_2 f_{12}|ij\rangle^{(s)} = \sum_{p'q'k} X_{ii}(\mathbf{r}_g)\langle j|f_{1g}|k\rangle\langle k|f_{1g}|j\rangle^{(s,ij)}, \tag{41}$$

where we have used the notation (s,ij) for the coupling corresponding to Eq. (11).

The first term in Eq. (40) is with different labels in the exchange and projection operators, and the use of QD for both of the two electronic coordinates should be avoided. We first subtract a large amount of the contribution through RI as

$$\langle ij|\hat{K}_1 f_{12}\hat{O}_1 f_{12}|ij\rangle^{(s)} = \langle ij|\hat{K}_1 f_{12}\hat{O}_1(1-\hat{P}_2)f_{12}|ij\rangle^{(s)} + \langle ij|\hat{K}_1 f_{12}\hat{O}_1\hat{P}_2 f_{12}|ij\rangle^{(s)}. \tag{42}$$

The second term of Eq. (42) is explicitly dealt with as Eq. (33). The first term is small and approximated by RI,

$$\langle ij|\hat{K}_1 f_{12}\hat{O}_1(1-\hat{P}_2)f_{12}|ij\rangle^{(s)} \overset{\mathrm{RI}}{\cong} \sum_p \langle i|\hat{K}_1|p\rangle\langle pj|f_{12}\hat{O}_1(1-\hat{P}_2)f_{12}|ij\rangle^{(s)}. \tag{43}$$

This approximation converges very quickly due to the small requirement of the maximum angular momentum in the RI basis L_{occ}. The approximation (43) bears close resemblance with the hybrid RI/ABS approach,[17] though the present method requires at most three-index objects. The error of the hybrid method is at least one order of magnitude smaller than the basis set truncation error,[17] and hence it is justified that the present approximation can be applied safely in the MP2-F12/B methods.

C. Integrals over the Slater-type geminal

As shown in Ref. 21, all types of integrals involving the Slater-type geminal can be calculated from the special function,

$$G_m(T,U) = \int_0^1 dt t^{2m}\exp\left[-Tt^2 + U\left(1-\frac{1}{t^2}\right)\right] \quad (m=-1,0,1,\ldots). \tag{44}$$

For nonnegative m, $G_m(T,U)$ reduces to $F_m(T)$ for electron repulsion integrals in the limit $U\to 0$. In practice, T ranges from 0 to infinity, while U is nonzero and usually less than a few hundreds with normal diffuse functions and geminal exponent. The partial integration leads to the upward and downward recurrence relations (URR and DRR),

$$G_m = \frac{1}{2T}[(2m-1)G_{m-1} + 2UG_{m-2} - e^{-T}], \tag{45}$$

$$G_m = \frac{1}{2U}[e^{-T} - (2m+3)G_{m+1} + 2TG_{m+2}], \tag{46}$$

stable for large T and U, respectively.

For large T, the transformation, $x=\sqrt{T}t\pm\sqrt{U}t^{-1}$, yields the relation

$$\int_{\pm\infty}^{\sqrt{T}\pm\sqrt{U}} e^{-x^2}dx = \int_0^1 (\sqrt{T}\mp\sqrt{U}t^{-2})e^{-(\sqrt{T}t\pm\sqrt{U}t^{-1})^2}dt, \tag{47}$$

that gives the explicit expressions of G_{-1} and G_0 in terms of the complementary error function,

$$G_{-1}(T,U) = \frac{e^{-T}}{4}\sqrt{\frac{\pi}{U}}[e^{\kappa^2}\,\mathrm{erfc}(\kappa) + e^{\lambda^2}\,\mathrm{erfc}(\lambda)], \tag{48}$$

$$G_0(T,U) = \frac{e^{-T}}{4}\sqrt{\frac{\pi}{T}}[e^{\kappa^2}\,\mathrm{erfc}(\kappa) - e^{\lambda^2}\,\mathrm{erfc}(\lambda)], \tag{49}$$

where

$$\kappa = -\sqrt{T} + \sqrt{U}, \tag{50}$$

$$\lambda = \sqrt{T} + \sqrt{U}. \tag{51}$$

The well-known asymptotic formula,

$$e^{\kappa^2}\,\mathrm{erfc}(\kappa) \cong \frac{1}{\kappa\sqrt{\pi}}\sum_{l=0}^{\infty}\frac{(-1)^l(2l-1)!!}{(2\kappa^2)^l}, \tag{52}$$

can be used for large κ^2.

For small T, $G_m(T,U)$ satisfies the differential relation as $F_m(T)$,

$$\frac{\partial^k}{\partial T^k}G_m(T,U) = (-1)^k G_{m+k}(T,U), \tag{53}$$

and the Maclaurin expansion formula is available,

$$G_m(T,U) = \sum_{k=0}^{\infty}\frac{(-T)^k}{k!}G_{m+k}(0,U). \tag{54}$$

A wide range of $G_m(0,U)$ in m is needed because the order of the expansion becomes about 60 at $T=10$. Equation (46) reduces to URR and DRR for $G_m(0,U)$,

$$G_m(0,U) = \frac{1}{2m+1}[1-2UG_{m-1}(0,U)], \tag{55}$$

$$G_m(0,U) = \frac{1}{2U}[1-(2m+3)G_{m+1}]. \quad (56)$$

For $U<5$, we used URR starting with

$$G_{-1}(0,U) = \frac{e^U}{2}\sqrt{\frac{\pi}{U}}\,\mathrm{erfc}(\sqrt{U}). \quad (57)$$

$G_m(0,U)$ is related with the incomplete gamma function, and that with an arbitrary m for $U \geqslant 5$ can be calculated by the continued fraction formula,

$$G_m(0,U) = \frac{1}{2}\left(\frac{1}{U+}\frac{m+(3/2)}{1+}\frac{1}{U+}\frac{m+(5/2)}{1+}\frac{2}{U+}\cdots\right). \quad (58)$$

It is known that the continued fraction can be calculated efficiently by the recurrences for the denominator and the numerator, and an analogous method for $F_m(T)$ was investigated.[32] One finds that Eqs. (55) and (56) are unstable when the magnitude of U is comparable with m. For instance, the substitution of Eq. (56) into itself,

$$G_m(0,U) = \frac{1}{2U}\left[1-\frac{2m+3}{2U}+O(U^{-2})\right], \quad (59)$$

suggests that there is a significant round-off error at $2U=2m+3$ for large U. Hence, $G_{m^*}(0,U)$ is calculated by Eq. (58) for $m^*=\mathrm{int}(U)$, and necessary functions with smaller and larger m are computed using URR and DRR for accurate $G_m(0,U)$.

The above formulas lead to three schemes from $s1$ to $s3$ for $G_m(T,U)$. $s1$ uses Eqs. (48) and (49) along with URR. The error function is related with $F_0(T)$, and this scheme is about twice as expensive as the computation of $F_m(T)$ for electron repulsion integrals with the corresponding URR. $s2$ consists of the Maclaurin expansion [Eq. (54)] and DRR [Eq. (46)]. DRR is not stable for small U and $G_m(T,U)$ should be calculated by Eq. (54) for all necessary m. This is $s3$ and is most expensive. $s1$ is usually cheaper than $s2$ especially for large T. In our earlier implementation, the schemes were selected by a rather empirical formula of the parameters, T and U. Here, we minimize the computational cost by employing a couple of look-up tables; one contains the upper bound of m up to which URR works in $s1$, while the other gives the maximum m where $s2$ is accurate downward. We used the ranges, $10^{-4} \leqslant T < 10$ and $10^{-4} \leqslant U < 10^3$ for the tables, and each digit is discretized into nine equal intervals, as $1\times10^{-4}, 2\times10^{-4}, \ldots, 1\times10^{-3}, 2\times10^{-3}, \ldots$. For $T<10^{-4}$, $s3$ is selected with the exception of a special case for $T=0$. In the tabulated range of T, we examine which scheme is optimal using the look-up tables. For $10<T\leqslant 15$, $s1$ is chosen if $U\leqslant 30$ otherwise $s2$ is used. For $15<T$, $s1$ suffices for the purpose. In this range, the value of the function becomes very small as U increases indicating that the correlation length of STG is negligibly small in comparison with the separation of orbital products. The present procedure makes about 90% of $G_m(T,U)$ be computed by $s1$. This is rather effective especially when the computation of $G_m(T,U)$ is the rate-determining step for a basis set without high angular momentum.

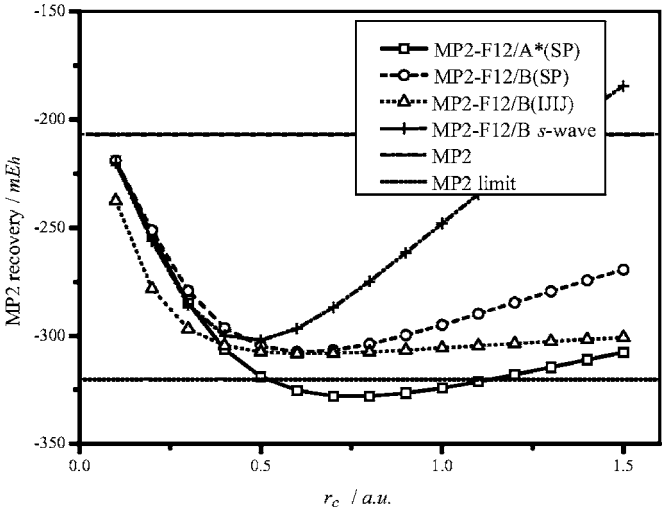

FIG. 1. Valence-shell correlated second-order Møller-Plesset correlation energy of the Ne atom as a function of the length scale parameter r_c in the aug-cc-pVDZ basis set.

III. RESULTS AND DISCUSSIONS

A. Preliminary calculations

1. r_c dependence and cusp conditions

In the previous work,[21] we used a fixed r_c based on MP2-F12/A*(SP) to avoid a nonlinear optimization of the STG exponent. Nevertheless, the optimum r_c can be altered by the inclusion of the Q term in the MP2-F12/B methods, which affects just the component quadratic to f_{12} in the Hylleraas energy functional. Figures 1 and 2 show the r_c dependence of the valence correlation energy of the Ne atom with aug-cc-pVDZ and aug-cc-pVTZ, respectively. In the aug-cc-pVDZ result, the MP2-F12/A*(SP) curve underlies the MP2 limit in the range $r_c=0.5-1.1$ and r_c of the minimum is larger than that of MP2-F12/B(SP). The MP2-F12/B(SP) energy is very close to the one of MP2-F12/B($IJIJ$) around $r_c=0.6$. This indicates that STG with the r_c is near universal

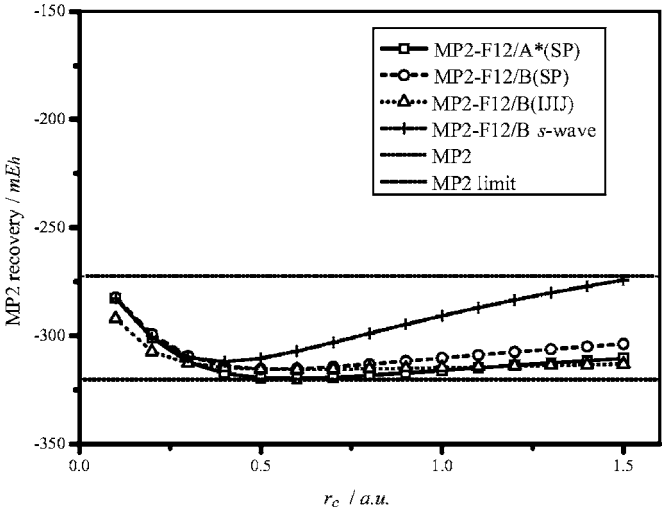

FIG. 2. Valence-shell correlated second-order Møller-Plesset correlation energy of the Ne atom as a function of the length scale parameter r_c in the aug-cc-pVTZ basis set.

TABLE II. MP2 energies for the Ne atom in the aug-cc-pVXZ sets (mE_h). The MP2 limit is −320.1 mE_h (Ref. 17).

Method	X=D	X=T	X=Q	X=5	X=6
MP2	−206.87	−272.52	−297.24	−307.97	−312.87
MP2-R12/2B[a]	−277.31	−305.61	−314.84	−318.15	−319.27
MP2-F12/2B[b]	−309.60	−315.77	−318.46	−319.48	−319.87
MP2-F12/B(SP)[c]	−307.27	−314.68	−317.98	−319.28	−319.79
MP2-F12/B($IJIJ$)[c]	−308.34	−315.56	−318.33	−319.43	−319.85

[a]With the *IJKL Ansatz* in Ref. 22.
[b]STG fit with six component GTGs. GTG exponents are optimized at each cardinal number (Ref. 22).
[c]Analytical STG with $r_c=2/3$.

to all of the valence correlations in the atom. Tew and Klopper reported the optimum exponent of STG, $\zeta=1.54$, based on the *IJKL Ansatz*.[22] This corresponds to the length scale parameter $r_c=1/\zeta\cong 0.65$ and agrees well with the present result. In order to see the importance of the p-wave cusp condition, we imposed the s-wave cusp condition to both of the singlet and triplet pairs as

$$\chi_{ij}^{(s)}(s\ \text{wave})=\hat{Q}_{12}f_{12}\{ij\}^{(s)}. \tag{60}$$

The s-wave only result is much inferior to the full use of the cusp conditions in the depth of the minimum and the insensitivity to r_c. The p-wave condition is secondary, that is, the leading term goes as $(L+1)^{-5}$ in the partial wave expansion, yet it is rather important actually. Our previous methods with the transcorrelated Hamiltonian[33–35] can fulfill only the s-wave cusp condition in the correlation factor. Hence, the geminal-based methods appear to be more advantageous though the transcorrelated methods coincide with MP2-F12 in most of the necessary integrals. It should be noted that the MP2-F12/B(SP) and MP2-F12/B($IJIJ$) curves are very close to each other in a wide range $r_c=0.4-0.7$ with aug-cc-pVTZ. We do not seek for optimum r_c for other molecules as such investigation has been already carried out to find the result less sensitive to the STG exponent.[22]

Henceforth we use $r_c=2/3$ for all calculations of the F12(SP) and F12($IJIJ$) methods. The parameter is slightly smaller than our previous choice based on MP2-F12/A*(SP) but would be more optimal for the MP2-F12/B method. In Table II, we compare the energies of the MP2, MP2-R12/2B, MP2-F12/2B, MP2-F12/B(SP), and MP2-F12/B($IJIJ$) methods for the Ne atom. We calculate all quantities involving two-electron integrals using numerical quadrature from orbital amplitudes, derivatives, and the three-center integrals over the operators, r_{1g}^{-1}, $f_{1g}r_{1g}^{-1}$, f_{1g}, $-(\nabla_1 f_{1g})$, $-(\nabla_1^2 f_{1g})-(\nabla_1 f_{1g})\cdot\nabla_1$, and $-(\nabla_1 f_{1g})\cdot(\nabla_1 f_{1g})$.[20] The integrals over $-(\nabla_1^2 f_{1g})$ and $-(\nabla_1 f_{1g})\cdot(\nabla_1 f_{1g})$ are linked with objects without a differential operator for STG.[21] The numerical quadrature in the MP2-F12/B(SP) and MP2-F12/B($IJIJ$) calculations is based on the "ultrafine" grid (see the later section), and there is no error in the numerical integrations up to the given decimal places. The MP2-R12/2B and MP2-F12/2B energies are taken from Ref. 22. They are based on the unitary invariant ($IJKL$) formulation along with the fitting STG with six-component GTGs. The STG exponent in MP2-F12/2B was optimized in each basis. All of the F12 energies are more accurate than MP2-R12/2B. The MP2-F12/2B and MP2-F12/B($IJIJ$) results are very similar for the atom, while there is a noticeable discrepancy with the aug-cc-pVDZ basis set. This is likely to be due to the somewhat different treatments of four-electron inte-

TABLE III. Convergence of the MP2-F12/B(SP) energy to the number of GTGs with aug-cc-pVXZ basis (mE_h). The MP2 limit is −320.1 mE_h (Ref. 17).

N	X=D	X=T	X=Q	X=5	X=6
0[a]	−206.87	−272.52	−297.24	−307.97	−312.87
1	−279.01	−293.61	−303.13	−309.32	−313.10
2	−303.09	−312.54	−315.64	−316.91	−317.77
3	−306.42	−314.36	−317.41	−318.80	−319.42
4	−307.10	−314.52	−317.83	−319.16	−319.71
5	−307.26	−314.55	−317.94	−319.25	−319.77
6	−307.30	−314.59	−317.97	−319.27	−319.79
10[b]	−307.25	−314.72	−317.97	−319.28	−319.79
Infinite[c]	−307.27	−314.68	−317.98	−319.28	−319.79

[a]The conventional MP2.
[b]Ten component GTG in Ref. 21.
[c]Analytical STG with $r_c=2/3$.

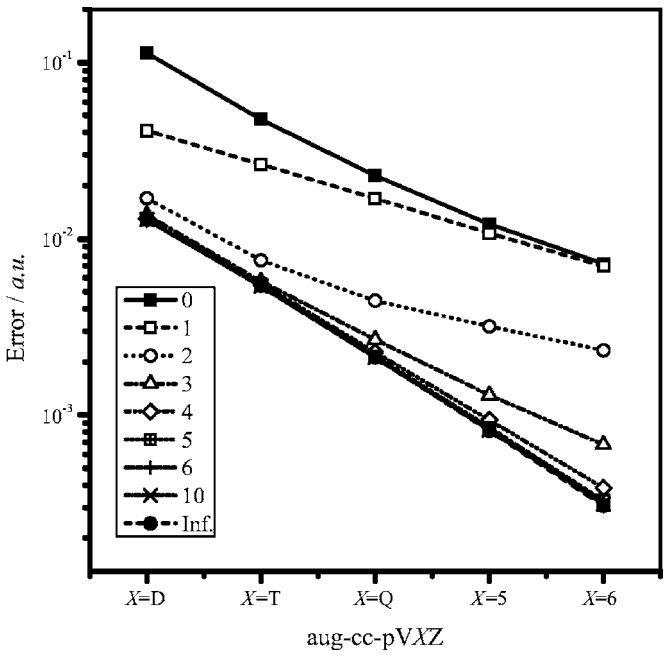

FIG. 3. The error in the MP2-F12/B(SP) correlation energy of N-component GTG fit as function of the cardinal number of the aug-cc-pVXZ basis set.

TABLE IV. Timings for the integrals of the MP2-F12/B(*SP*) method in the aug-cc-pV*XZ* basis (CPU seconds). The total CPU time for integrals is $t_N + t_F$ (see the text).

	N	*X*=D	*X*=T	*X*=Q	*X*=5	*X*=6
t_N	1	0.51	0.67	1.16	2.09	3.19
	2	1.04	1.61	2.69	4.91	7.59
	3	1.60	2.49	4.22	7.56	12.09
	4	2.16	3.36	5.77	10.28	15.88
	5	2.72	4.30	7.34	13.01	20.82
	6	3.50	5.31	9.06	16.00	25.74
	10[a]	6.26	10.17	17.46	30.23	49.80
	Infinite[b]	1.63	2.35	3.52	5.04	4.77
t_F	Fundamental	2.07	6.06	17.82	50.56	130.88

[a]Ten component GTG in Ref. 21.
[b]Analytical STG with $r_c=2/3$.

grals and the optimization of the correlation factor. The MP2-F12/B(*SP*) energies are slightly higher than those of MP2-F12/2B and MP2-F12/B(*IJIJ*) as discussed in the previous section. But we mainly use MP2-F12/B(*SP*) as a standard method because of its nice features in Table I.

2. STG versus GTG fit

Tew and Klopper determined the exponents and coefficients of *N*-component GTGs to represent STG approximately for $N=1-6$.[22] In Table III, we show the MP2-F12/B(*SP*) energies based on the GTGs along with the ten-component GTG used in the previous work.[21] In all calculations, r_c of the reference STG is kept 2/3. Figure 3 shows the error of the energy referring to the near MP2 limit $-0.3201\ E_h$. Indeed a single GTG ($N=1$) lowers the energy with a small basis set such as aug-cc-pVDZ, but the curve merges with the conventional MP2 ($N=0$) as cardinal number increases. This deficiency with a large basis is attributed to the difficulty of GTG to describe the cusps that need basis functions with high angular momentum. Nevertheless the augmentation of the expansion of GTG improves the result markedly. Especially the curves with $N>4$ are very close to the analytic Slater (N=infinite). The result with aug-cc-pV6Z indicates that at least $N=3$ is needed to make the fitting error less than 1 mE_h.

TABLE V. Definition of grids.

	Coarse	Medium	Medium (old)	Fine	Ultrafine
n_r	20	32	48	48	64
n_ω	128	288	288	512	800
n_{total}	2560	9216	13 824	24 576	51 200

Table IV lists timings for the integrals in the *N* GTG and STG calculations based on the ultrafine grid. The total CPU time for the integrals is given as a sum of the individual value t_N plus the timing for the fundamental operation t_F, $t_{N,\text{total}}=t_N+t_F$, for each *N*. The fundamental operation is the component independent of *N* and consists mainly of the increments of angular momentum indices and the build of integrals. The present integral code for GTG integrals is coincident with that for STG except for the computation of special functions analogous to $G_m(T,U)$. Thus the rest of t_F is linear and quadratic to *N* to generate the special functions. t_F is obtained from the second order polynomial fitting of the timing statistics of all GTG calculations. Although STG does not require the integrals over f_{1g}^2, t_N for the analytic STG (N=infinite) corresponds to the time for $G_m(T,U)$ approximately. The CPU time for N=infinite is comparable to that for GTG with $N=3$ up to QZ, and the performance increases for larger cardinal numbers. It was shown that $N\geqslant 3$ is needed for a satisfactory result in the previous section. Thus the use of analytic STG is advantageous over GTG-fit especially for accurate calculations with an extended basis, even though the fundamental operation gets to dominate the integral evaluation with the size of the basis.

3. Convergence of numerical integration

The MP2-F12 methods have been implemented into the GELLAN program system[36] recently. In the new implementa-

TABLE VI. MP2 energies of urea (NH_2CONH_2) in the different grids (mE_h).

		Grid					
Basis set	Method	Coarse	Medium	Medium (old)	Fine	Ultrafine	Limit
X=D	MP2[a]	−684.48	−683.78	−683.79	−683.81	−683.81	−683.81[b]
	MP2-F12/A*(*SP*)	−911.01	−909.33	−909.36	−909.38	−909.39	···
	MP2-F12/B(*SP*)	−887.61	−885.82	−885.85	−885.87	−885.88	···
X=T	MP2[c]	−827.17	−826.36	−826.38	−826.39	−826.39	−826.39[b]
	MP2-F12/A*(*SP*)	−919.23	−918.35	−918.38	−918.41	−918.42	···
	MP2-F12/B(*SP*)	−911.53	−910.62	−910.65	−910.69	−910.70	···
X=Q	MP2[c]	−877.41	−876.56	−876.57	−876.59	−876.59	−876.59[b]
	MP2-F12/A*(*SP*)	−919.58	−918.37	−918.40	−918.43	−918.44	···
	MP2-F12/B(*SP*)	−917.10	−915.71	−915.75	−915.77	−915.78	···

[a]Numerical MP2 method in Ref. 20.
[b]The limiting values obtained from the usual MP2 of analytical electron repulsion integrals.
[c]There are small deviations from the numbers in Ref. 27 by 20 μE_h. This is due to the symmetrization in the Fock assembly with the numerical quadrature introduced in the new program.

TABLE VII. Valence-shell MP2 correlation energies of small molecules in the aug-cc-pV*X*Z basis sets (mE_h).

Method	System[a]	X=D	X=T	X=Q	X=5	X=6	Limit[b]
A*(*SP*)	$CH_2(^1A_1)$	−152.12	−155.80	−155.90	−155.87	−155.88	−155.9
	H_2O	−300.56	−300.65	−300.47	−300.43	−300.45	−300.5
	NH_3	−261.82	−264.60	−264.51	−264.43	−264.43	−264.5
	HF	−323.68	−319.69	−319.54	−319.58	−319.64	−319.7
	N_2	−416.09	−420.84	−420.96	−420.95	−420.95	−421.0
	CO	−401.29	−403.90	−403.91	−403.87	−403.88	−403.9
	Ne	−327.37	−319.26	−319.54	−319.77	−319.93	−320.1
	F_2	−619.05	−611.40	−611.13	−611.28	−611.43	−611.7
B(*SP*)	$CH_2(^1A_1)$	−148.12	−154.47	−155.45	−155.72	−155.82	−155.9
	H_2O	−290.19	−297.67	−299.50	−300.11	−300.33	−300.5
	NH_3	−254.89	−262.51	−263.85	−264.22	−264.35	−264.5
	HF	−308.63	−315.77	−318.27	−319.15	−319.50	−319.7
	N_2	−405.85	−417.13	−419.50	−420.39	−420.72	−421.0
	CO	−389.82	−399.95	−402.41	−403.30	−403.66	−403.9
	Ne	−307.27	−314.68	−317.98	−319.28	−319.79	−320.1
	F_2	−590.73	−603.90	−608.53	−610.39	−611.15	−611.7
B(*IJIJ*)	$CH_2(^1A_1)$	−150.39	−154.67	−155.48	−155.72	−155.82	−155.9
	H_2O	−291.42	−297.75	−299.55	−300.14	−300.34	−300.5
	NH_3	−257.00	−262.63	−263.88	−264.23	−264.36	−264.5
	HF	−309.32	−316.06	−318.42	−319.22	−319.53	−319.7
	N_2	−409.29	−417.38	−419.59	−420.43	−420.74	−421.0
	Co	−392.33	−400.12	−402.47	−403.33	−403.67	−403.9
	Ne	−308.34	−315.56	−318.33	−319.43	−319.85	−320.1
	F_2	−592.31	−604.60	−608.90	−610.56	−611.22	−611.7

[a]Geometrical parameters are taken from Ref. 17.
[b]Estimate of the R12 methods taken from Ref. 12.

tion, we define "coarse," "medium," "fine," and ultrafine grids based on the polar coordinates as listed in Table V in addition to the option to specify the numbers of radial and angular grid points, n_r and n_ω explicitly. The "medium" (old) is the default grid used in the original F12 program with a different platform. Table VI shows the MP2 and MP2-F12 energies of the different grids with aug-cc-pV*X*Z for the urea molecule as an example. The optimized geometries are at the MP2/aug-cc-pVTZ level,[37] and are same as used in Ref. 28. The number of the total grid points is 204 800 for ultrafine after the application of the $C2$ point group symmetry. The numerical MP2 energies are saturated up to the final decimal places with the fine grid. The MP2-F12 energies seem to converge somewhat slower than numerical MP2, but the difference between the fine and ultrafine grids is small (approximately 10 μE_h). The new choice of the medium grid is therefore considered to give MP2-F12 energies at least more accurate than 0.1 mE_h sufficing for ordinary purposes. The new medium grid is smaller than the old one in the radial points but with comparable accuracies. It is noted that the main source of the error in a numerical integration is the deformation of the integrand around an atom by the fuzzy cell. Thus it is expected that the error scales approximately linearly with respect to the number of atoms.

B. Small molecules

We apply the MP2-F12 methods to the selection of the small molecules given in Ref. 12 for comparison with the performance of the linear-r_{12} *Ansatz*. The geometrical parameters optimized at the all-electron correlated CCSD(T)/cc-pCVQZ level[38] are taken from Ref. 17. The aug-cc-pV*X*Z (X=D, T, Q, 5, and 6) and aug-cc-pCV*X*Z (X=D, T, Q, and 5) basis sets are used for valence-shell and all-electron correlated calculations, respectively. The medium grid is employed henceforward in this paper.

The results of the MP2-F12/A*(*SP*), B(*SP*), and B(*IJIJ*) methods are listed in Tables VII (valence-shell correlated) and VIII (all-electron correlated). The average MP2 recoveries of the results are summarized in percentage in Table IX and are plotted in Fig. 4 (valence-shell correlated) and Fig. 5 (all-electron correlated).

As for the valence-shell correlated calculations, MP2-R12/2B with aug-cc-pVDZ gives a result almost equivalent to the conventional MP2 with aug-cc-pVTZ. The situation of R12 methods is improved by the augmentation of basis according to the different convergences of $(L_{max}+1)^{-3}$ for MP2 and $(L_{max}+1)^{-7}$ for MP2-R12/2B. Furthermore, the MP2-F12 methods increase the accuracy from R12 by the amounts equivalent to increasing the cardinal number by one in the entire range in agreement with the recent observation.[22,28] It is also noted that the difference between MP2-F12/B(*SP*) and MP2-F12/B(*IJIJ*) is one order of magnitude smaller than the basis set truncation error. Hence it is quite reasonable to use the MP2-F12/B(*SP*) method for valence-shell correlated calculations. As there is a cancellation of the errors from neglecting the exchange commutator and basis set truncation, MP2-F12/A*(*SP*) gives surprisingly better average recoveries ranging from 99.4% to 99.8%. Both errors go

TABLE VIII. All electron MP2 correlation energies of small molecules in the aug-cc-pCV*X*Z basis sets (mE_h).

Method	System[a]	X=D	X=T	X=Q	X=5	Limit[b]
A*(*SP*)	$CH_2(^1A_1)$	−203.91	−208.38	−209.54	−209.72	−209.9
	H_2O	−356.02	−360.43	−361.84	−362.01	−362.1
	NH_3	−316.25	−321.31	−322.54	−322.69	−322.9
	HF	−379.85	−382.75	−384.28	−384.48	−384.6
	N_2	−524.46	−533.55	−536.21	−536.68	−536.9
	CO	−508.92	−516.38	−518.98	−519.40	−519.7
	Ne	−384.18	−385.87	−387.61	−387.91	−388.1
	F_2	−730.95	−736.86	−739.80	−740.32	−740.6
B(*SP*)	$CH_2(^1A_1)$	−198.96	−207.73	−209.38	−209.70	−209.9
	H_2O	−344.55	−358.78	−361.37	−361.92	−362.1
	NH_3	−308.08	−320.11	−322.20	−322.63	−322.9
	HF	−363.92	−380.66	−383.78	−384.38	−384.6
	N_2	−511.80	−531.70	−535.59	−536.53	−536.9
	CO	−495.29	−514.44	−518.39	−519.26	−519.7
	Ne	−363.51	−383.60	−387.16	−387.89	−388.1
	F_2	−700.87	−733.00	−738.93	−740.16	−740.6
B(*IJIJ*)	$CH_2(^1A_1)$	−203.04	−208.34	−209.49	−209.73	−209.9
	H_2O	−351.29	−359.59	−361.49	−361.94	−362.1
	NH_3	−313.70	−320.85	−322.33	−322.66	−322.9
	HF	−372.31	−381.56	−383.89	−384.41	−384.6
	N_2	−522.27	−533.15	−535.84	−536.58	−536.9
	Co	−505.25	−515.83	−518.64	−519.34	−519.7
	Ne	−374.29	−384.69	−387.29	−387.91	−388.1
	F_2	−717.59	−734.81	−739.16	−740.20	−740.6

[a]Geometrical parameters are taken from Ref. 17.
[b]Estimate of the R12 methods taken from Ref. 12.

as $(L_{max}+1)^{-5}$. However, it is clear that correlation energy is overshot significantly for a small basis set if we use the A*(*IJIJ*) *Ansatz*.

In the all-electron correlated case, the percentage of the recovery with MP2-R12/2B is better than the valence-shell correlated result in each corresponding cardinal number. The F12 methods certainly lead to a gain over the linear-r_{12} though the difference between MP2-F12/B(*SP*) and MP2-F12/B(*IJIJ*) is non-negligible for the smallest basis set aug-cc-pCVDZ (as large as 2.2%). The recoveries of the MP2-F12/B methods with this basis are lacking for the amount of MP2-R12/2B with the aug-cc-pCVTZ basis set. Beyond aug-cc-pCVDZ, the augmentation of the core polarization functions mitigates these features to grant a gain of accuracy equivalent to increasing the basis set of the MP2-R12/2B calculation by one cardinal number again.

TABLE IX. Average recoveries of the valence (aug-cc-pV*X*Z) and all-electron (aug-cc-pCV*X*Z) MP2 correlation energies of the selection of small molecules (%).

				F12		
Basis	X	MP2[a]	R12/2B[a]	A*(*SP*)	B(*SP*)	B(*IJIJ*)
aug-cc-pV*X*Z	D	72.0	89.2	99.94	96.25	96.86
	T	88.8	96.4	99.96	98.91	99.01
	Q	94.8	98.7	99.96	99.60	99.64
	5	97.3	99.5	99.96	99.84	99.86
	6	98.3	99.8	99.98	99.93	99.94
aug-cc-pCV*X*Z	D	70.7	91.6	98.18	94.86	96.94
	T	89.1	98.1	99.44	99.00	99.25
	Q	95.3	99.4	99.88	99.77	99.81
	5	97.5	99.8	99.95	99.93	99.94

[a]Reference 12.

C. Reaction enthalpies

We investigate the performance of the MP2-F12/B methods on reaction enthalpies for the set of 21 molecules and 16

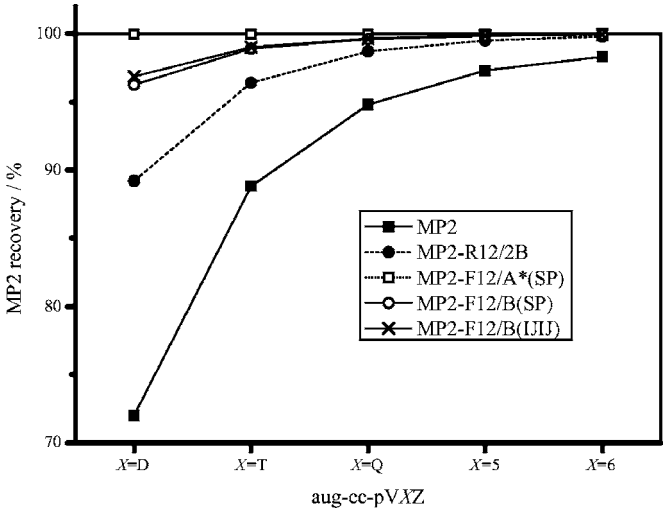

FIG. 4. The average recovery of the valence-shell correlated second-order Møller-Plesset correlation energy in the aug-cc-pV*X*Z basis set.

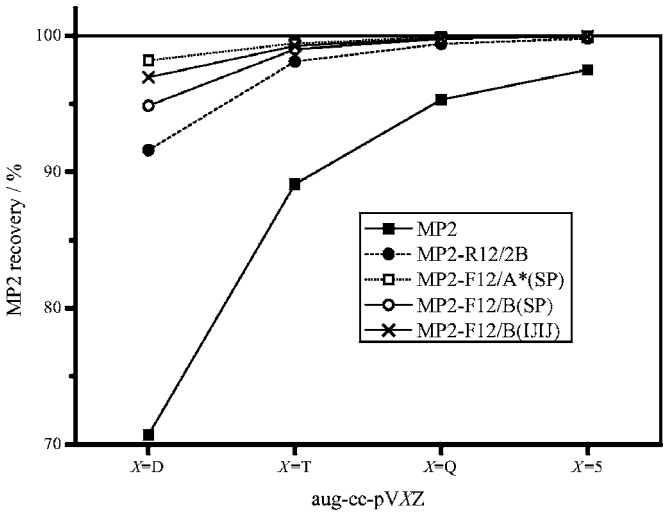

FIG. 5. The average recovery of the all-electron correlated second-order Møller-Plesset correlation energy in the aug-cc-pV*X*Z basis set.

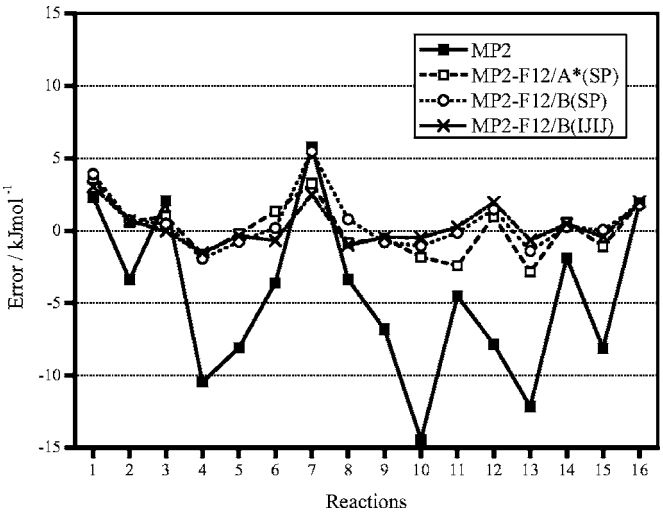

FIG. 6. Errors of MP2 contribution to reaction enthalpies in kJ/mol in the aug-cc-pVDZ basis set.

reactions studied by Manby *et al.*[26] and Warner and Manby.[37] Table X lists the correlation energies of the MP2-F12/A*(*SP*), B(*SP*), and B(*IJIJ*) methods with aug-cc-pV*X*Z (*X*=D, T, and Q). It is considered the MP2-F12/2*A(loc)/aug-cc-pV5Z energies[26] are close to the CBS limits. The numbers are tabulated as reference data. Figures 6–8 show the errors of the MP2 and MP2-F12 contributions to the enthalpies of the 16 chemical reactions. The numbering of the reactions is same as those in Refs. 26 and 37. The mean and maximum errors are listed in Table XI. The mean error of the MP2-F12 methods ranges from 1/4 to 1/6 of the MP2 one at any cardinal number. The maximum errors with aug-cc-pVDZ are less than 4 kJ/mol for MP2-F12/A*(*SP*) and MP2-F12/B(*IJIJ*). Although this basis might be too small for quantitative calculations, the accuracies suffice for many applications in chemistry. The largest errors in the F12 results are observed in reactions (1) and (7), which involve C_2H_2. The maximum error obtained at the MP2-F12/A*(*SP*)/aug-cc-pVTZ level is 0.73 kJ/mol (approximately 0.2 kcal/mol) in agreement with the result of MP2-F12/2*A(loc).[26] However, the inclusion of the exchange commutator in B(*SP*) and B(*IJIJ*) slightly worsens the situation for

TABLE X. MP2 correlation energies of molecules for chemical reactions in the aug-cc-pV*X*Z basis sets (mE_h). Geometrical parameters are same as in Ref. 37.

	F12/A*(*SP*)			F12/B(*SP*)			F12/B(*IJIJ*)			
Molecule	*X*=D	*X*=T	*X*=Q	*X*=D	*X*=T	*X*=Q	*X*=D	*X*=T	*X*=Q	Reference[a]
H_2	−34.11	−34.22	−34.23	−33.01	−34.04	−34.20	−33.27	−34.07	−34.20	−34.21
CH_4	−215.48	−219.09	−219.10	−210.43	−217.62	−218.67	−213.18	−217.85	−218.70	−218.87
NH_3	−261.86	−264.64	−264.55	−254.94	−262.55	−263.89	−257.05	−262.67	−263.92	−264.28
H_2O	−300.87	−300.97	−300.80	−290.51	−298.00	−299.82	−291.74	−298.08	−299.88	−300.41
C_2H_2	−337.55	−345.71	−346.23	−330.78	−343.06	−345.22	−336.03	−343.61	−345.32	−346.00
C_2H_4	−365.29	−372.44	−372.78	−357.55	−369.82	−371.92	−362.73	−370.31	−371.99	−372.48
C_2H_6	−402.28	−409.57	−409.66	−393.48	−406.88	−408.83	−398.91	−407.34	−408.89	−409.34
CO	−402.85	−405.46	−405.48	−391.41	−401.53	−403.99	−393.91	−401.69	−404.05	−405.05
H_2CO	−445.71	−449.08	−449.10	−433.07	−445.01	−447.69	−435.98	−445.20	−447.75	−448.64
CH_3OH	−481.75	−485.48	−485.39	−467.80	−481.26	−484.02	−471.13	−481.48	−484.08	−484.86
H_2O_2	−570.18	−570.61	−570.34	−551.00	−564.93	−568.42	−553.53	−565.10	−568.53	−569.67
H_2CCO	−601.55	−609.29	−609.60	−586.46	−604.10	−607.73	−591.79	−604.53	−607.84	−608.98
C_2H_4O	−641.01	−648.79	−649.00	−624.66	−643.55	−647.23	−630.49	−643.97	−647.31	−648.43
CH_3CHO	−633.28	−640.58	−640.70	−617.00	−635.30	−638.89	−622.34	−635.67	−638.97	−640.03
C_2H_5OH	−670.18	−677.93	−677.93	−652.70	−672.52	−676.17	−658.43	−672.92	−676.25	−677.23
HNCO	−649.95	−656.60	−656.72	−633.18	−650.76	−654.61	−637.77	−651.04	−654.68	−655.99
$HCONH_2$	−679.35	−685.35	−685.38	−661.28	−679.44	−683.34	−666.11	−679.72	−683.41	−684.66
CO_2	−685.34	−688.72	−688.74	−665.51	−682.05	−686.29	−669.13	−682.27	−686.40	−687.90
HCOOH	−716.14	−719.66	−719.56	−694.75	−712.87	−717.20	−698.62	−713.08	−717.29	−718.79
NH_2CONH_2	−909.33	−918.35	−918.37	−885.82	−910.62	−915.71	−892.71	−911.04	−915.80	−917.41
$HCOOCH_3$	−901.11	−908.39	−908.35	−876.27	−900.40	−905.61	−882.38	−900.78	−905.72	−907.50

[a]The result at the MP2-F12/2*A(loc)/aug-cc-pV5Z level in Ref. 26.

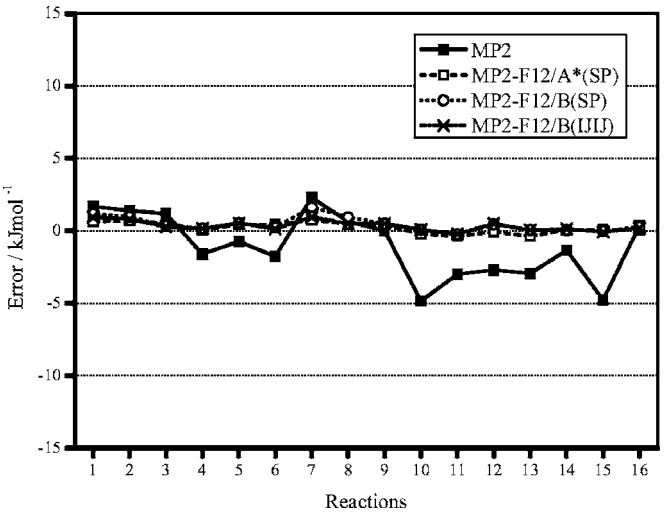

FIG. 7. Errors of MP2 contribution to reaction enthalpies in kJ/mol in the aug-cc-pVTZ basis set.

the present selection of the reactions. At any rate, the maximum errors are reduced by factors of 3–6 from MP2.

IV. CONCLUSION

We have proposed a novel hybrid QD/RI method for the exchange commutator in explicitly correlated MP2-F12 theory. In the method, a certain class of four-electron integrals can be computed explicitly by QD and the others are treated by the partial use of the RI approximation. The method is well suited with the STG correlation factor avoiding the computation of the additional integrals over f_{12}^2. For the special function $G_m(T,U)$ required for the STG integrals, there are three different schemes dependent on the variables, T and U, and the order of m. We have maximized the efficiency of the routine for $G_m(T,U)$ by introducing look-up tables to select the optimum scheme for a given set of variables. We concluded that the use of an analytic STG is advantageous based on the comparison with GTG calculations in timing and accuracy.

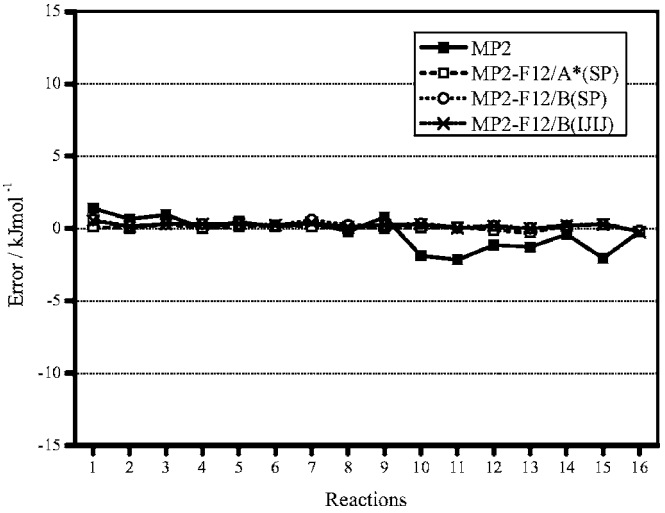

FIG. 8. Errors of MP2 contribution to reaction enthalpies in kJ/mol in the aug-cc-pVQZ basis set.

TABLE XI. Mean and maximum absolute errors in reaction enthalpies (kJ/mol).

				F12		
Basis	Error	X	MP2	A*(SP)	B(SP)	B($IJIJ$)
aug-cc-pVXZ	Mean	D	6.04	1.54	1.32	1.03
		T	1.95	0.35	0.48	0.38
		Q	0.88	0.14	0.27	0.24
	Maximum	D	14.43	3.57	5.49	3.05
		T	4.84	0.73	1.62	0.95
		Q	2.16	0.34	0.60	0.53

We also investigated the *SP*, *IJIJ*, and *IJKL Ansätze* theoretically and numerically. The SP *Ansatz* supplies the unitary invariance that *IJIJ* misses, retaining the simplicity of the implementation. It was shown that all *Ansätze* perform almost similarly especially beyond the aug-cc-p(C)VDZ basis. MP2-F12/A*(*SP*) generally outperforms MP2-F12/B(*SP*) and MP2-F12/B(*IJIJ*) for the selection of the molecules and chemical reactions in this work. However, it is likely that the contribution of the exchange commutator is crucial for some energetics. More comprehensive surveys will make this aspect clearer. The model reactions investigated in this work do not include the contribution of core-electron correlation, which is non-negligible for comparison with experimental data in conjunction with more sophisticated correlation models. Our individual result indicates that the inclusion of core-electron correlation makes the contrast between the MP2 and MP2-F12 methods even clearer.[39]

ACKNOWLEDGMENTS

The author acknowledges H.-J. Werner for providing the MP2/aug-cc-pVTZ geometries. He also thanks Y. Kawashima and J. Franz for reading the manuscript carefully.

[1] T. Kato, Commun. Pure Appl. Math. **10**, 151 (1957).
[2] R. T Pack and W. Byers-Brown, J. Chem. Phys. **45**, 556 (1966).
[3] W. Kutzelnigg and J. D. Morgan III, J. Chem. Phys. **96**, 4484 (1992).
[4] E. A. Hyleraas, Z. Phys. **54**, 347 (1929).
[5] S. F. Boys, Proc. R. Soc. London, Ser. A **258**, 402 (1960).
[6] K. Singer, Proc. R. Soc. London, Ser. A **258**, 412 (1960).
[7] K. C. Pan and H. F. King, J. Chem. Phys. **56**, 4667 (1972).
[8] L. Adamowicz and A. J. Sadlej, J. Chem. Phys. **69**, 3992 (1978).
[9] K. Szalewicz, B. Jeziorski, H. J. Monkhorst, and J. G. Zabolitzky, J. Chem. Phys. **78**, 1420 (1983).
[10] W. Kutzelnigg, Theor. Chim. Acta **68**, 445 (1985).
[11] W. Kutzelnigg and W. Klopper, J. Chem. Phys. **94**, 1985 (1991).
[12] W. Klopper and C. C. M. Samson, J. Chem. Phys. **116**, 6397 (2002).
[13] T. H. Dunning, Jr., J. Chem. Phys. **90**, 1007 (1989).
[14] R. A. Kendall, T. H. Dunning, Jr., and R. J. Harrison, J. Chem. Phys. **96**, 6769 (1992).
[15] D. E. Woon and T. H. Dunning, Jr., J. Chem. Phys. **103**, 4572 (1995).
[16] F. R. Manby, J. Chem. Phys. **119**, 4607 (2003).
[17] W. Klopper, J. Chem. Phys. **120**, 10890 (2004).
[18] S. Ten-no and F. R. Manby, J. Chem. Phys. **119**, 5358 (2003).
[19] E. F. Valeev, Chem. Phys. Lett. **395**, 190 (2004).
[20] S. Ten-no, J. Chem. Phys. **121**, 117 (2004).
[21] S. Ten-no, Chem. Phys. Lett. **398**, 56 (2004).
[22] D. P. Tew and W. Klopper, J. Chem. Phys. **123**, 074101 (2005).
[23] A. J. May, E. Valeev, R. Polly, and F. R. Manby, Phys. Chem. Chem. Phys. **7**, 2710 (2005).
[24] C. Villani and W. Klopper, J. Phys. B **38**, 2555 (2005).
[25] D. P. Tew and W. Klopper, J. Chem. Phys. **125**, 094302 (2006).

[26] F. R. Manby, H.-J. Werner, T. B. Alder, and A. J. May, J. Chem. Phys. **124**, 094103 (2006).
[27] S. Fournais, M. Hoffmann-Ostenhof, T. Hoffmann-Ostenhof, and T. Ø. Sørensen, Commun. Math. Phys. **255**, 183 (2005).
[28] W. Klopper, F. R. Manby, S. Ten-no, and E. F. Valeev, Int. Rev. Phys. Chem. **25**, 427 (2006).
[29] S. Ten-no, in *Explicitly Correlated Wavefunctions*, edited by E. A. G. Armour, J. Franz, and J. Tennyson [Collaborative Computational Project on Continuum States of Atoms and Molecules (CCP2), Daresbury, 2006].
[30] W. Klopper, Chem. Phys. Lett. **186**, 583 (1991).
[31] W. Klopper, W. Kutzelnigg, H. Müller, J. Noga, and S. Vogtner, Top. Curr. Chem. **203**, 21 (1999).
[32] F. Harris, Int. J. Quantum Chem. **23**, 1469 (1983).
[33] S. Ten-no, Chem. Phys. Lett. **330**, 169 (2000).
[34] O. Hino, Y. Tanimura, and S. Ten-no, J. Chem. Phys. **115**, 7865 (2001).
[35] O. Hino, Y. Tanimura, and S. Ten-no, Chem. Phys. Lett. **353**, 317 (2002).
[36] GELLAN, A hierarchical quantum chemistry program, Nagoya University, 2006.
[37] H.-J. Werner and F. R. Manby, J. Chem. Phys. **124**, 054114 (2006).
[38] K. L. Bak, J. Gauss, P. Jørgensen, J. Olsen, T. Helgaker, and J. F. Stanton, J. Chem. Phys. **114**, 6548 (2001).
[39] S. Ten-no (unpublished).